J Solid State Electrochem (2012) 16:3611–3619
DOI 10.1007/s10008-012-1795-3

ORIGINAL PAPER

Porous alumina membranes with branched nanopores as templates for fabrication of Y-shaped nanowire arrays

Leszek Zaraska · Elżbieta Kurowska · Grzegorz D. Sulka · Marian Jaskuła

Received: 20 March 2012 / Accepted: 3 June 2012 / Published online: 24 June 2012

Abstract Porous anodic alumina membranes with Y-branched and double-branched nanopores were fabricated by the stepwise reduction of anodizing potential during the second step of anodization carried out in 0.3 M oxalic acid. The process of nanoporous layer formation and influence of anodizing parameters on structural features of as-obtained anodic aluminum oxide (AAO) membranes were discussed in detail. The pore rearrangement process occurring after the potential decrease was investigated on the basis of the current density vs. time curves, and results were correlated with the field-emission scanning electron microscope images of the pore bottoms taken after different anodizing durations. It was found that the reorganization of nanopores begins after 600 and 500 s from the time of the potential reduction to 42 and 30 V and the process seems to be completed after about 900 and 800 s, respectively. The through-hole AAO membranes were used as templates for the fabrication of gold and polystyrene nanowires via electrochemical deposition and simple immersing in the polymer solution, respectively. The arrays of hierarchically branched nanowires were synthesized, and the dimensions of nanowires were consistent with the shape and structure of used AAO templates.

Keywords Anodization · Branched nanopores · Y-shaped nanowires · Electrodeposition

L. Zaraska (✉) · E. Kurowska · G. D. Sulka · M. Jaskuła
Department of Physical Chemistry and Electrochemistry,
Faculty of Chemistry, Jagiellonian University,
Ingardena 3,
30-060 Krakow, Poland
e-mail: zaraska@chemia.uj.edu.pl

Introduction

Recently, a strong trend towards miniaturization of electronic devices could be observed, therefore, all disciplines of nanotechnology have become the most popular scientific areas in both academic science and industry [1, 2]. Among numerous nanomaterials fabricated over the last decades, 1D nanostructures, such as nanowires and nanotubes are subjects of great research interest not only due to their unusual physical and chemical properties, but also because of their potential applications in modern nanodevices [3]. Although great progress has been made in fabrication of simple 1D nanostructures over the last few years [4–6], the synthesis of multifunctional nanodevices often requires more complex nanostructures and, thus, many research groups are working on development of methods for nanomanufacturing.

Among many strategies, the use of porous anodic aluminum oxide (AAO) membranes as templates for nanofabrication seems to be the most popular, cheapest and simplest way for synthesis of nanowires [7–10], nanotubes [8, 11], nanodots [12, 13], or even sophisticated 3D nanoarrays with precisely controlled dimensions [14–16]. A number of reports on fabrication of metallic nanowires and nanotubes by cathodic electrodeposition inside nanochannels of AAO templates can be found, but most of them refer to the simplest and linear nanomaterials with uniform diameters [14].

Nowadays, big attention is focused on fabrication of hierarchically structured nanomaterials, e.g., Y-junction and multibranched nanowires and nanotubes that can be potentially used as device interconnectors [17, 18]. Nanoporous alumina membranes with branched nanopores can be also obtained by using a simple anodizing procedure. A few strategies have been already reported [19–25].

Wang et al. have synthesized a large-size, multibranched AAO template by anodizing in a phosphate-based solution, at the constant current density of 1.3 $A dm^{-2}$ and 5 °C [20]. It was found that the diameter of pores on the outer surface of the oxide layer ranges from 150 to 220 nm, and each main channel has many branches whose width is about 100–120 nm. The authors suggested that the formed complex structure of AAO can be ascribed to the unstable growth of oxide film at the initial stage of the process [20]. On the other hand, Zakeri et al. reported the synthesis of nonlinear nanopores in alumina films by anodizing of different geometric shaped substrates [21]. It was shown that a control over the orientation of nanopores can be accomplished by controlling the geometric shape of aluminum substrates on which alumina layers are grown. A simple model that predicts the shape and orientation of nonlinear nanopores grown on different shaped substrates was also published [21]. Zhang et al. proposed another method for the fabrication of hyper-branched nanoporous structures by sequences of potential- and current-controlled anodizations performed in an oxalic acid solution [22].

The most common and widely used strategy to fabricate AAO membranes with branched nanopores is changing the anodizing potential during the second step of anodization [19]. It is widely recognized that both, pore diameter and interpore distance, depend linearly on applied potential with a proportionality constant of about 1.29 and 2.5 nm V^{-1}, respectively [23]. The reduction of the anodizing potential by a factor of $1/\sqrt{2}$ results in the formation of Y-branched pores [24, 25]. Two-, three-, and four-generation Y-branched (hierarchically branched) pores can be also obtained by further sequential reduction of anodizing potentials by the same factor. Using the same methodology, multiply branched nanopores are formed as a result of the reduction of the anodizing potential by a factor of $1/\sqrt{n}$, where n is a number of branches [24]. Up to now, there are only a few papers on fabrication of branched metallic nanowires by electrodeposition inside the pores of AAO templates [22, 24–29].

Here, we present results on formation of through-hole AAO membranes with branched nanopores. The process of nanoporous layer formation and influence of anodizing parameters on structural features of as-obtained membranes are discussed in detail. A special emphasis is put on the investigation of the pore rearrangement process after the reduction of anodizing potential and correlation of current density curves with the field-emission scanning electron microscope (FE-SEM) images of the pore bottoms taken after different anodizing durations. In addition, some results on fabrication of Y-branched nanowire arrays are also presented.

Experimental

Fabrication of AAO templates with branched pores

The high purity (99.999 %) annealed aluminum foil (Goodfellow), 0.5 mm thick was used as a starting material. Al substrates with dimensions of $25 \times 5 \times 0.5$ mm were degreased in acetone and ethanol and electrochemically polished in a mixture of perchloric acid (60 wt%) and ethanol (1:4 vol.) at a constant voltage of 20 V for 30 s at 0 °C (Fig. 1a).

The nanoporous alumina layers were prepared on the Al surface by simple two-step self-organized anodization carried out in 0.3 M oxalic acid at 20 °C. The first anodization was performed under the constant potential of 60 V for 1 h (Fig. 1b). The oxide layers formed on the Al surface were removed by chemical etching in a mixture of 6 wt% H_3PO_4 and 1.8 wt% H_2CrO_4 at 45 °C for 12 h (Fig. 1c). After that, the second anodization was performed at 60 V (Fig. 1d). In order to obtain Y-branched nanopores, the applied potential was reduced to 42 V after 120 min (Fig. 1e) and maintained for different periods of time (5, 10, 20, and 30 min). It allows to investigate the oxide growth rate at the reduced potential. In order to form AAO membranes with two level branched pores, after 30 min of anodizing at 42 V, the applied potential was reduced to 30 V and the duration of this step was 10, 20, 30, and 40 min (Fig. 1h). All anodizations were performed in a simple electrochemical cell with vigorous magnetic stirring, thermostated by a powerful circulating system (Thermo Haake, DC10-K15). A working surface area of the aluminum sample (about 0.5 cm^2) was selected by insulation of the rest of the sample with an acid resistant paint. A Pb plate served as the cathode and the distance between both electrodes was about 3 cm. After anodizations, samples were rinsed with water and dried. The remaining Al substrate was chemically removed in a saturated $HgCl_2$ solution (Fig. 1f and i). After that, the chemical etching of the continuous oxide layer at the pore bottoms, called "barrier layer", was carried out in a 5 wt% H_3PO_4 solution at 35 °C (Fig. 1g and j). AAO membranes were put on a microscopic glass and dipped into the acid solution for a specified period of time. By monitoring the duration of the pore-opening process, membranes with a different pore diameters were obtained. After the pore opening, AAO membranes were cleaned in water then ethanol and dried.

Synthesis of nanowires

As-prepared through-hole AAO membranes were used as templates for electrochemical fabrication of Y-shaped metallic nanowire arrays. Before the electrodeposition, a thin Au conducting layer was sputtered at the bottom side of the membrane. Au nanowire arrays were synthesized by a simple DC galvanostatic electrodeposition at the constant current density

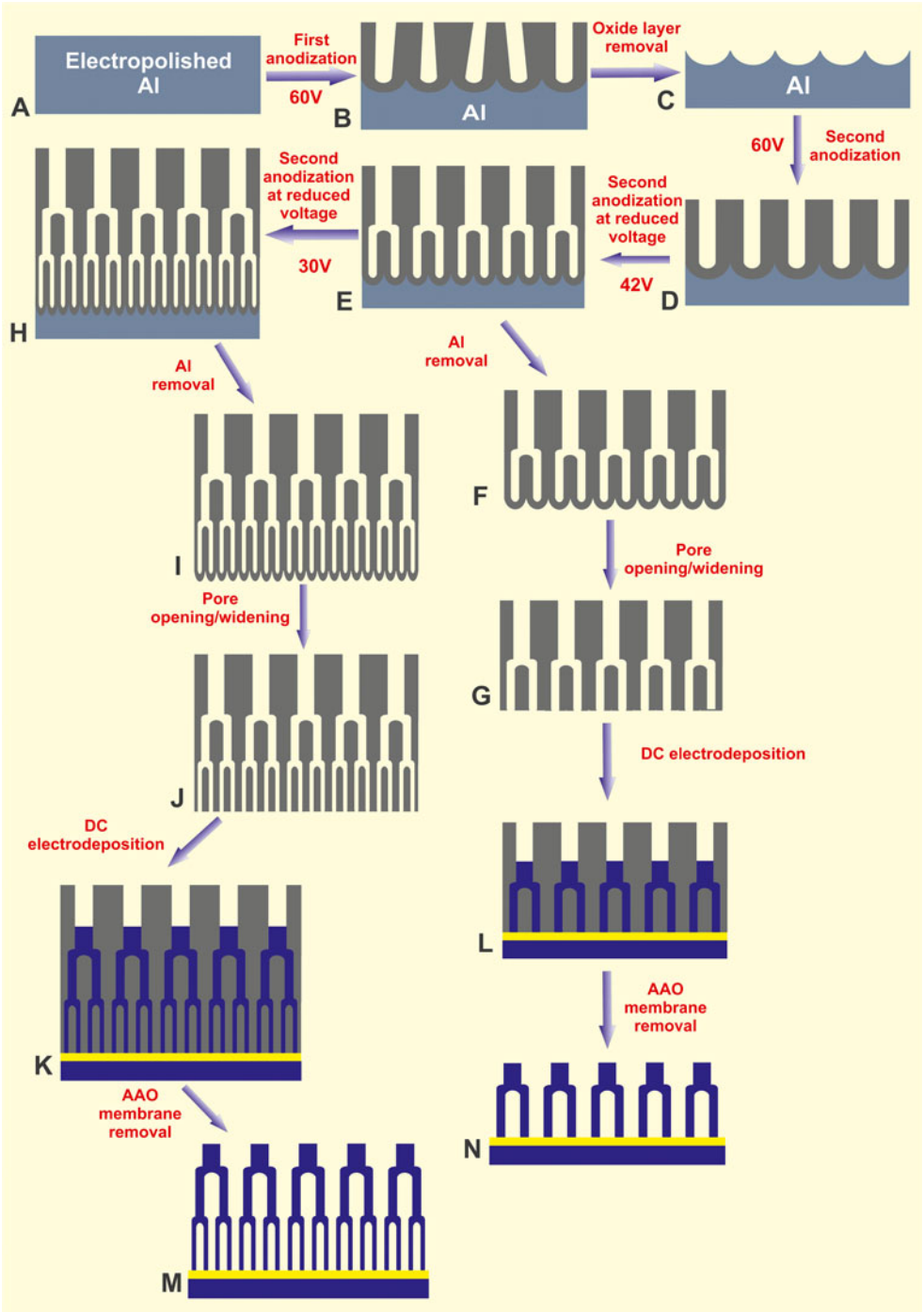

Fig. 1 Schematic representation of the anodization procedure used for fabrication of AAO membranes with Y-branched or two level branched nanochannels and branched metallic nanowire arrays

of 1 mA cm^{-2} in a commercially available electrolyte (Auruna® 5000; Au content, 7 gdm^{-3}; Fig. 1k and l). All electrodeposition experiments were performed in a typical three-electrode cell with the AAO membrane as a working electrode and Pt plates as a counter and reference electrodes using a Reference 3000 potentiostat (Gamry Instruments). After the electrodeposition process, samples were rinsed with water then ethanol and dried. In order to release the fabricated nanowires, AAO templates were chemically removed in a 1 M NaOH solution at room temperature for 60 min (Fig. 1m and n). Polystyrene nanowire arrays were obtained by immersing AAO templates in a 1.5 wt% solution of polystyrene in chloroform.

Characterization

The morphology of AAO templates and nanowire arrays was studied with a FE-SEM/energy dispersive X-ray

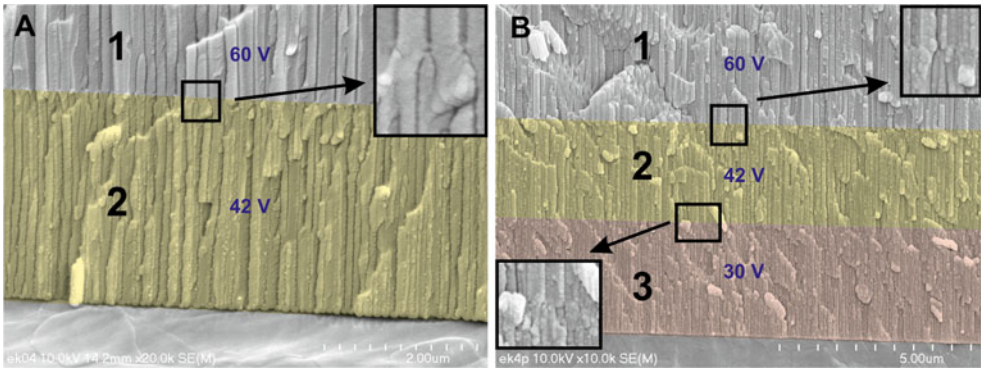

Fig. 2 Cross-sectional FE-SEM images of nanoporous AAO membranes with Y-branched (**a**) and two-level-branched (**b**) nanopores. The anodization at 60 V was carried out for 120 min. The duration of anodizing at the reduced potential of 42 V (**a** and **b**) and 30 V (**b**) was 30 min

spectrometer (EDS; Hitachi S-4700 with a Noran System 7). The composition of nanowires was confirmed by EDS analyses. The characteristic parameters of AAO membranes such as oxide layer thickness, interpore distance and pore diameter were calculated on the basis of SEM images by using the scanning probe image processor WSxM v.12.0 [30], ImageJ software [31], and an executable paper [32].

Results and discussion

The cross-sectional views of AAO templates with Y-branched and two level-branched nanopores are presented in Fig. 2a and b, respectively. In both cases, long and parallel nanochannels can be easily recognized. As can be seen, when the anodizing potential is reduced from 60 to 42 V each pore is divided into two smaller channels (yellow areas "2" in the SEM images), and in that way the Y-branched pore structure is obtained. A subsequent reduction of the anodizing potential from 42 to 30 V leads to a second division of nanochannels (pink area "3" in the SEM image) and formation of the template with hierarchically branched nanopores. It is well known that the thickness of oxide layer grown on aluminum is almost linearly proportional to the duration of the anodization process [33]. Therefore, a length of nanochannels can be easily controlled by adjusting the anodizing time. The influence of anodizing conditions on the rate of porous oxide growth was discussed in detail in our previous work [33]. Unfortunately for the AAO templates with hierarchically-branched pores, the dependence between the thickness of the porous oxide layer and the duration of the anodizing step after the reduction of the anodizing potential, is more complicated.

In order to get deeper insight into the oxide growth rates after subsequent reductions of the anodizing potential, the thicknesses of oxide layers grown at the reduced potentials were estimated from FE-SEM images for different process durations. Then, the oxide growth rates for different time periods were calculated. The relationships between the oxide growth rate and different time periods for anodizations carried out at the reduced potentials of 42 and 30 V are shown in Fig. 3a and b, respectively.

It can be seen that the reduction of potential affects considerably the rate of oxide growth. In particular, just after the potential reductions, the oxide growth rates are much lower than those observed during anodizing at fixed potentials of 42 and 30 V (red dash lines). For the process performed at the reduced potential, the oxide growth rate significantly increases with increasing anodizing time. In both cases, the stable values of the oxide growth rate, closed to the values observed for potentiostatic anodizations under 42 and 30 V, are reached after about 30 min. To explain this

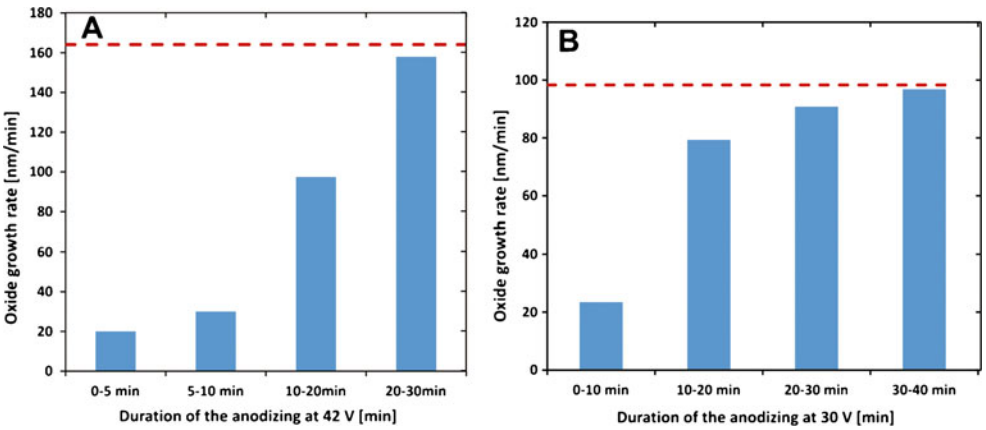

Fig. 3 Oxide growth rates for different anodizing periods after the potential reduction to 42 V (**a**) and 30 V (**b**)

tendency, the current density vs. anodizing time curve is shown in Fig. 4.

The shape of the current–potential curve, after the anodizing potential reduction, is consistent with those reported previously by Takahashi et al. [19] and O'Sullivan and Wood [34]. Both observations about the curve shape and formation mechanism leading to the Y-branched channels could be explained in terms of the most reliable field-assisted mechanism of the porous layer growth [35]. It should be noted that the barrier layer thickness is linearly dependent on the anodizing potential with a proportionality constant of about 1.04 nm V^{-1} [34]. After 2 h of anodizing under 60 V, the applied potential was reduced to 42 V. As a result of the potential reduction, the current density decreased to almost negligible values, due to the fact that the electric field across the barrier oxide layer is too small, and remained almost constant for about 500 s. Consequently, the low rate of oxide growth, observed during the first 10 min of anodizing under 42 V, is the result of low current densities. It can be seen that after 300 s of anodizing under the reduced voltage (Fig. 4a), the bottom side of the AAO layer looks still the same as after anodizing under 60 V [33]. This fact is also confirmed by an average cell diameter shown in Fig. 6 which is close to the cell diameter of the AAO layer formed by anodizing under 60 V. After some time, the thickness of the barrier layer starts to decrease due to the progressive

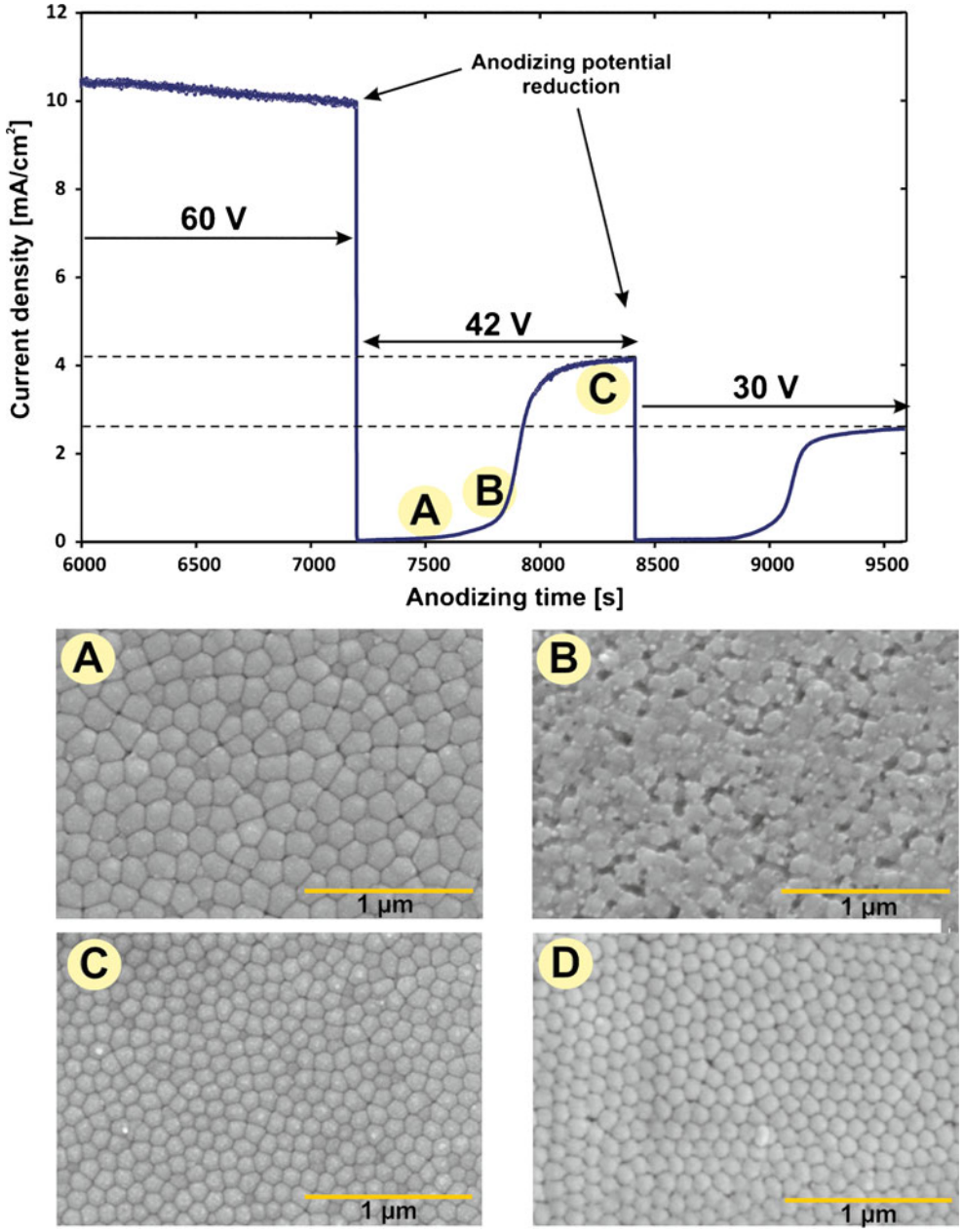

Fig. 4 The relationship between the current density and duration of the second anodizing step before and after reduction of the anodizing potential from 60 to 42 V together with FE-SEM images of the bottom side of AAO membranes after 300 s (**a**), 600 s (**b**), and 1,200 s (**c**) anodizing under 42 V, and after two-step anodization under 42 V without any potential changes (**d**)

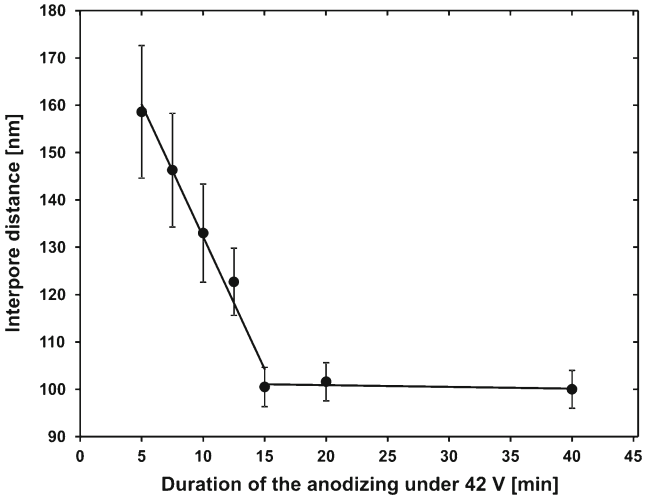

Fig. 5 The relationship between the cell size estimated from the bottom side of the AAO membrane and duration of the anodizing step after the potential reduction from 60 to 42 V

dissolution of the oxide layer in the electrolyte, so the electric field gradually increases. As a result, a gradual increase in the current density and oxide growth rate can be observed after about 600 s of anodizing under 42 V. In evidence of that, some disordered areas at the bottom side of the AAO with a partially dissolved barrier layer can be noticed (see Fig. 4b). When the current density increases, the process of the pore rearrangement begins and new cells are formed [19]. As a consequence of this process, a decrease in the average cell diameter (see Fig. 5) and increase in the oxide growth rate are observed (see Fig. 3).

In addition, the current density begins to stabilize and the rearrangement of pores seems to be completed after about 900 s. At this stage of the anodizing process, the size of hexagonal cells is similar to the cell size observed in AAO membranes formed under 42 V without any potential changes (about 105 nm).

It is well known that the best pore order in AAOs, anodized in oxalic acid solutions, can be observed at potentials closed to 40 V (self-ordering regime) [23]. As can be clearly seen, the degree of pore order, after reorganization of the structure, is much higher than before the pore rearrangement. However, the regularity of pore arrangement is still not as good as observed for AAOs formed by anodizing under 42 V without any potential changes (compare Fig. 4c and d). This phenomenon can be attributed to the fact that concaves formed on the Al surface during the first anodization carried out at 60 V were arranged in a different way than is required for the anodization at 42 V.

In order to fabricate a second level of branches in AAO layers, after 20 min of anodization at 42 V, the anodizing potential was reduced to 30 V. As a result of the potential reduction, a significant decrease in current density, to almost negligible values, and lower rates of the oxide growth were observed (Fig. 3b). For this case, the rearrangement of the pores, indicated by the current density increase, begins at about 500 s after the application of the reduced potential. Consequently, for higher current densities the increase in the oxide growth rate is also observed (Fig. 3b). The reorganization is completed after about 800 s of anodizing at 30 V, and the alumina growth rate reaches a destination value (dash line).

In order to obtain a through-hole AAO membrane a procedure of pore opening by chemical etching in a phosphoric acid should be performed. It is noteworthy

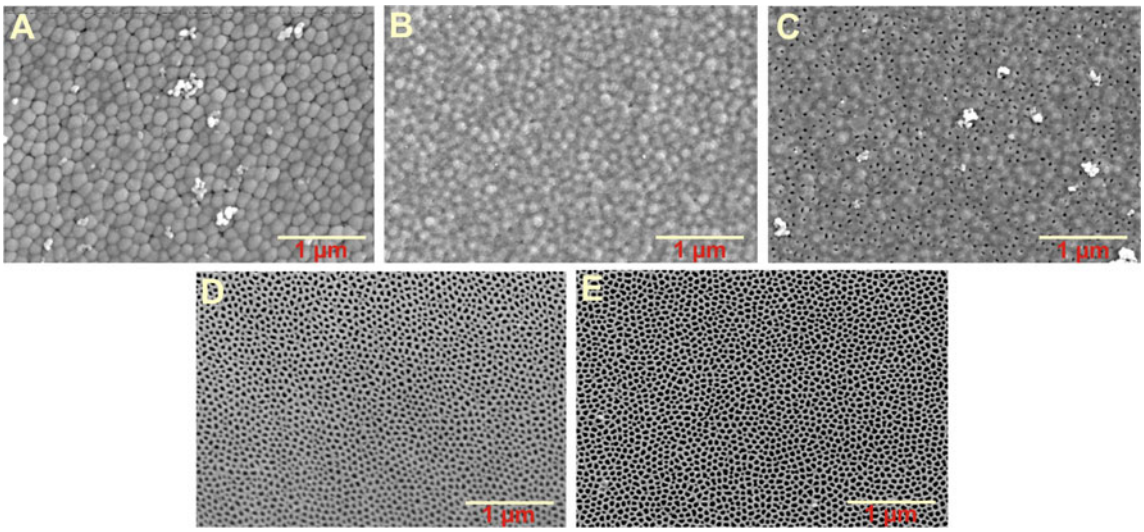

Fig. 6 FE-SEM images of bottom sides of AAO membranes with two level branched pores before the pore opening procedure (**a**) and after 20 min (**b**), 25 min (**c**), 30 min (**d**), and 40 min (**e**) of chemical etching in a 5 wt% H_3PO_4 solution at 35 °C

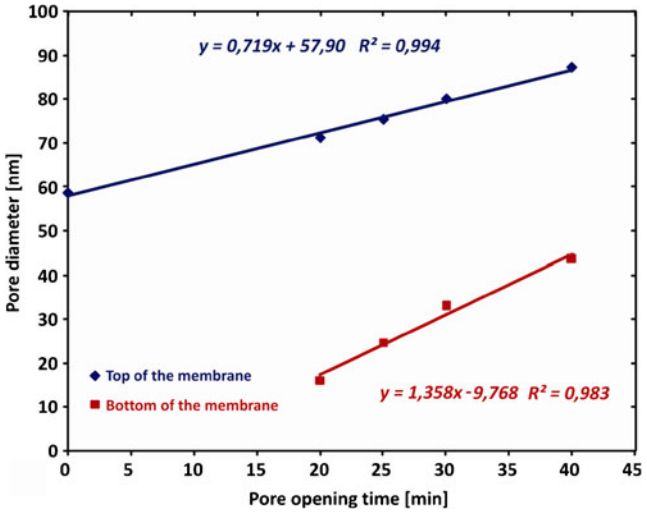

Fig. 7 The relationship between the pore diameter and duration of the pore opening procedure for nanoporous membranes with two level branched channels

that the thickness of the barrier layer strongly depends on anodizing conditions, especially on the applied potential. Moreover, the etching rate of AAO is strongly affected by the concentration of H_3PO_4 and etching temperature. Thus, the procedure of pore opening, always associated with pore widening, should be optimized carefully. Figure 6 shows FE-SEM images of the bottom side of AAO membranes with two level branched nanopores formed by anodizing of the high purity Al foil in 0.3 M oxalic acid at 20 °C. The duration of the anodizing under 60, 42, and 30 V was 7,200, 1,200, and 1,800 s, respectively. The pore opening procedure was carried out in 5 wt% H_3PO_4 at 35 °C.

It is clearly visible that after 20 min of pore opening pores are still closed (Fig. 6b) but, the pore bottoms are smoother when compared with those observed for the membrane before the chemical etching in phosphoric acid (Fig. 6a). This is a result of an isotropic thinning of the barrier layer by the acidic etchant. After 25 min of pore opening, some holes can be visible, but the majority of pores are still closed (Fig. 6c). The complete removal of the barrier layer is achieved after 30 min of etching and the average diameter of opened pores is about 30 nm (Fig. 6d). When the duration of the pore opening/widening process is extended to 40 min, the average pore diameter increases to about 45 nm (Fig. 6e).

It should be noted that the pore opening procedure carried out in a phosphoric acid solution widens also the nanopore mouths. The adhesion of the top side of the AAO membrane to the microscopic glass results in a slightly lower etching rate at the top of the alumina template than at the bottom side that was directly exposed to the acidic solution. Therefore, widening of the pore diameter at the top side of the AAO layer proceed a little bit slower than at the bottom side (Fig. 7).

As was mentioned before, pore and cell dimensions in AAO depend linearly on anodizing potential and, thus, it is obvious that these parameters should be considerably larger at the top side than at the bottom side of the AAO membrane. To illustrate this point, FE-SEM images of top and bottom sides of the nanoporous AAO membrane with Y-branched nanochannels after pore opening are shown in Fig. 8.

The average pore diameter and cell size estimated for both sides of the AAO membranes having one- or two-level-branched pores are collected in Table 1. Both types of alumina membranes with Y-branched and two-level-branched nanopores were used as templates for fabrication of Au and polystyrene nanowire arrays. The gold nanowire arrays fabricated by cathodic electrodeposition inside AAO membranes with branched nanopores are shown in Fig. 9a and b. The template with Y-branched channels was synthesized by the two-step anodization in 0.3 M oxalic acid at 20 °C, and the duration of the process at the reduced potential of 42 V was 10 min. After 10 min of electrochemical deposition, a uniform array of ultra short Y-shaped Au nanowires was formed (Fig. 9a).

The diameters of the trunk of the nanowire and branches roughly correspond to the dimensions of the Y-branched nanochannels of the AAO template used for electrodeposition.

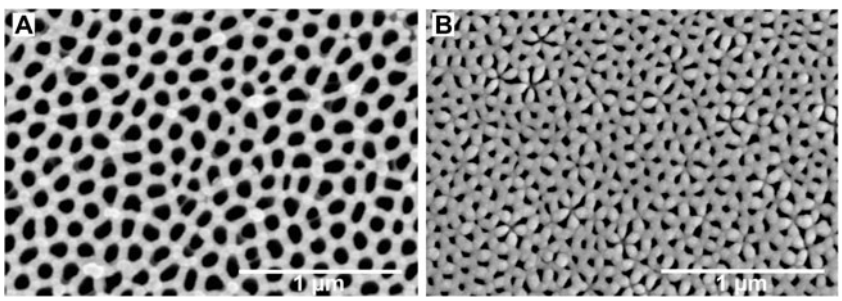

Fig. 8 FE-SEM images of the top (**a**) and bottom (**b**) sides of the AAO membrane with Y-branched pores after 50 min of pore opening in 5 wt% H_3PO_4 at 35 °C

Table 1 Pore diameters and cell dimensions for AAO membranes with hierarchically branched nanopores formed by anodizing in 0.3 M oxalic acid at 20 °C and after the pore opening/widening procedure

Type of the membrane	Pore opening conditions	Pore diameter (nm)		Cell diameter (nm)	
		Top view	Bottom view	Top view	Bottom view
AAO with Y-branched nanopores	5 wt% H_3PO_4; 35 °C; 50 min	~90	~65	~140	~100
AAO with two level branched nanopores	5 wt% H_3PO_4; 35 °C; 40 min	~90	~40	~140	~70

The prepared Y-branched nanowire array was mechanically stable and easy to handle that makes it possible to be used as a nanostructured electrode in modern applications such as catalysis, sensors and current collectors. The FE-SEM image of hierarchically branched Au nanowires grown by electrodeposition at 1 mA cm^{-2} for 20 min is shown in Fig. 9b. Also in this case, the dimensions of branched Au nanowires are consistent with the shape of alumina nanochannels used as a template.

Another method that involved pore filling of the AAO template with a polymer was also used for fabricating branched polymer nanowire arrays. The through-hole AAO membranes with Y-branched and two level branched nanopores were immersed into the solution of polystyrene in chloroform for the desired amount of time and allowed to dry in air at room temperature. The FE-SEM images of fabricated and released from the AAO template Y-branched and two-level branched polystyrene nanowires are shown in Fig. 9c and d, respectively. The prepared polystyrene nanowires precisely reproduce the dimensions and shape of pores of the AAO templates used for their fabrication.

Conclusions

In summary, the two-step self-organized anodization with the stepwise reduction of the applied potential is a simple and effective method for fabrication of anodic alumina membranes with Y-branched and two-level-branched nanochannels. Just after the reduction of anodizing potential, a significant decrease in both current density and oxide growth rates were observed. It was found that for anodizations carried out in 0.3 M $H_2C_2O_4$ the process of pore rearrangement is completed after about 900 and 800 s from the time at which the potential was reduced to 42 and 30 V, respectively. In order to obtain through-hole alumina membranes, a simple pore opening procedure carried out in 5 wt% H_3PO_4 should be performed. The pore diameter at the top and bottom sides of the AAO membrane depends linearly on the etching time. As-prepared anodic alumina membranes can be easily employed as templates for the fabrication of Y-branched and two-level-branched gold nanowires by cathodic electrodeposition. The uniform filling of AAO templates with polystyrene results in the formation of branched polymer nanowires that precisely reproduce the dimensions and shape of nanopores.

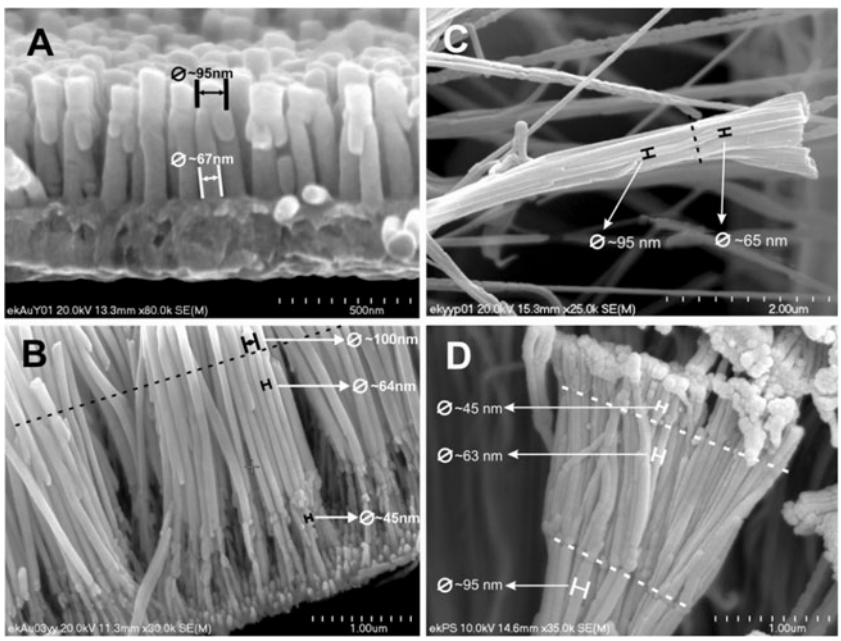

Fig. 9 FE-SEM images of Y-branched Au (**a**) and polystyrene (**c**) nanowires and two-level-branched Au (**b**) and polystyrene (**d**) nanowires after the removal of the alumina template

Acknowledgments The research was partially carried out with the equipment purchased thanks to the financial support of the European Regional Development Fund in the framework of the Polish Innovation Economy Operational Program (contract no. POIG.02.01.00-12-023/08).

This work was performed with assistance of the PL-Grid project, contract number: POIG.02.03.00-00-007/08-00, website: www.plgrid.pl. The project is co-funded by the European Regional Development Fund as part of the Innovative Economy Program.

The SEM imaging was performed in the Laboratory of Field Emission Scanning Electron Microscopy and Microanalysis at the Institute of Geological Sciences, Jagiellonian University, Poland.

References

1. Bhushan B (ed) (2008) Springer handbook of nanotechnology, 2nd edn. Springer, Berlin
2. Chen S (ed) (2010) Nanomanufacturing. American Scientific, New York
3. Iwamoto M, Kaneto K, Mashiko S (eds) (2003) Nanotechnology and nano-interface controlled electronic devices. Elsevier, Amsterdam
4. Iijima S (1991) Nature 354:56–58
5. Morales AM, Lieber CM (1998) Science 279:208–211
6. Pan ZW, Dai ZR, Wang ZL (2001) Science 291:1947–1949
7. Yin AJ, Li J, Jian W, Bennett AJ, Xu JM (2001) Appl Phys Lett 79:1039–1041
8. Fu J, Cherevko S, Chung CH (2008) Electrochem Commun 10:514–518
9. Sulka GD, Brzózka A, Zaraska L, Jaskuła M (2010) Electrochim Acta 55:4368–4376
10. Li R, Chen QW, Hu XY, Wang MS, Wang CW, Zhong H (2012) RCS Adv 2:2250–2253
11. Yu Y, Kant K, Shapter JG, Addai-Mensah J, Losic D (2012) Microporous Mesoporous Mater 153:131–136
12. Jung JS, Kim EM, Chae WS, Malkinski LM, Lim JH, O'Connor C, Jun JH (2008) Bull Korean Chem Soc 29:2169–2171
13. Kondo T, Miyazaki H, Nishio K, Masuda H (2011) J Photoch Photobio A 221:199–203
14. Sulka GD, Zaraska L, Stępniowski WJ (2011) Encyclopedia of nanoscience and nanotechnology, vol 11, 2nd edn. American Scientific, CA, pp 261–349
15. Moyen E, Santinacci L, Masson L, Sahaf H, Mace M, Assaud L, Hanbucken M (2012) Int J Nanotechnol 9:246–259
16. Tsukamoto T, Ogino T (2012) J Electrochem Soc 159:C155–C159
17. Li J, Papadopoulos C, Xu J (1999) Nature 402:253–254
18. Papadopoulos C, Rakitin A, Li J, Vedeneev AS, Xu JM (2000) Phys Rev Lett 85:3476–3479
19. Takahashi H, Nagayama M, Akahori H, Kitahara A (1973) J Electron Microsc 22:149–157
20. Wang H, Wang HW, Zeng P (2008) Key Eng Mater 373–374:252–255
21. Zakeri R, Watts C, Wang H, Kohli P (2007) Chem Mater 19:1954–1963
22. Zhang J, Day CS, Carroll DL (2009) Chem Commun 2009:6937–6939
23. Sulka GD (2008) In: Eftekhari A (ed) Nanostructured materials in electrochemistry. Wiley, Weinheim, pp 1–116
24. Meng G, Jung YJ, Cao A, Vajtai R, Ajayan PM (2005) Proc Natl Acad Sci U S A 102:7074–7078
25. Xu L, Yuan Z, Zhang X (2006) Chin Sci Bull 51:2055–2058
26. Gao T, Meng G, Zhang J, Sun S, Zhang L (2002) Appl Phys A 74:403–406
27. Choi J, Sauer G, Nielsch K, Wehrspohn RB, Gösele U (2003) Chem Mater 15:776–779
28. Kong LB, Lu M, Li MK, Li HL (2003) J Mater Sci Lett 22:701–702
29. Biswas KG, El Matbouly H, Rawat V, Schroeder JL, Sands TD (2009) Appl Phys Lett 95:073108/1–4
30. Horcas I, Fernández R, Gómez-Rodríguez JM, Colchero J, Gómez-Herrero J, Baro AM (2007) Rev Sci Instrum 78:013705/1–8
31. Image J. National Institute of Mental Health, Bethesda, MD, USA, http://rsb.info.nih.gov/ij
32. Ciepiela E, Zaraska L, Sulka GD (2012) Lect Notes Comput Sci 7136:240–251
33. Zaraska L, Sulka GD, Jaskuła M (2011) J Solid State Electrochem 15:2427–2436
34. O'Sullivan JP, Wood GC (1970) Proc R Soc Lond A 317:511–543
35. Parkhutik VP, Shershulsky VI (1992) J Phys D Appl Phys 25:1258–1263